Multimodal recording of brain activity in term newborns during photic stimulation by near-infrared spectroscopy and electroencephalography

Martin Biallas
Ivo Trajkovic
Cornelia Hagmann
Felix Scholkmann
Carmen Jenny
Lisa Holper
Andreas Beck
Martin Wolf

Multimodal recording of brain activity in term newborns during photic stimulation by near-infrared spectroscopy and electroencephalography

Martin Biallas,[a,b] Ivo Trajkovic,[a,b] Cornelia Hagmann,[a] Felix Scholkmann,[a] Carmen Jenny,[a] Lisa Holper,[a,c] Andreas Beck,[d] and Martin Wolf[a]

[a]University Hospital Zurich, Biomedical Optics Research Laboratory, Division of Neonatology, CH-8091 Zurich, Switzerland
[b]University of Zurich and ETH Zurich, Institute for Biomedical Engineering, CH-8093 Zurich, Switzerland
[c]University of Zurich and ETH Zurich, Institute of Neuroinformatics, CH-8057 Zurich, Switzerland
[d]University of Basel, Core Program of Structural Biology and Biophysics, Biozentrum, CH-4056 Basel, Switzerland

Abstract. In this study 14 healthy term newborns (postnatal mean age 2.1 days) underwent photic stimulation during sleep on two different days. Near-infrared spectroscopy (NIRS) and electroencephalography (EEG) was acquired simultaneously. The aims of the study were: to determine (i) the sensitivity and (ii) the repeatability of NIRS to detect the hemodynamic response, (iii) the sensitivity and (iv) the repeatability of EEG to detect a visual evoked potential (VEP), (v) to analyze optical data for the optical neuronal signal, and (vi) to test whether inadequate stimulation could be reason for absent hemodynamic responses. The results of the study were as follows. (i) Sensitivity of NIRS was 61.5% to detect hemodynamic responses; (ii) their reproducibility was 41.7%. A VEP was detected (iii) in 96.3% of all subjects with (iv) a reproducibility of 92.3%. (v) In two measurements data met the criteria for an optical neuronal signal. The noise level was $9.6 \cdot 10^{-5}\%$ change in optical density. (vi) Insufficient stimulation was excluded as reason for absent hemodynamic responses. We conclude that NIRS is an promising tool to study cognitive activation and development of the brain. For clinical application, however, the sensitivity and reproducibility on an individual level needs to be improved. © *2012 Society of Photo-Optical Instrumentation Engineers (SPIE).*
[DOI: 10.1117/1.JBO.17.8.086011]

1 Introduction

Hemodynamic indicators resulting from near-infrared spectroscopy (NIRS) are used to assess neural activity. This ability to investigate neural activity offers a useful and interesting opportunity to assess the neural basis of visual cognitive development in infants. This is of special interest in preterm infants, as many of them develop visual cognitive impairment in later childhood.[1] This visual impairment is thought to result from injury to the posterior visual pathway in the context of periventricular white matter lesions,[2] even in the absence of major neuromotor impairment.[3] NIRS with the ability to detect hemodynamic responses (HR) and potential optical neuronal signals might offer an optimal instrumentation for assessing the visual cognitive development. The possibility of early detection of aberration in the development of the visual pathway in this population is important in order to select infants who are at high risk for visual impairment and would benefit from neuroprotective interventions. However, before functional NIRS can be used in clinical practice, important aspects such as reproducibility, sensitivity, specificity, and predictive values have to be determined.[4] In adults, variable degrees of NIRS sensitivity have been described, but little is known on repeatability of the

signals.[5,6] Further, while relatively few and controversial information on HR in response to visual stimulation in newborn infants has been reported in the literature,[7–11] information on reproducibility or potential optical neuronal signals in newborns is lacking. Previous NIRS studies measuring activation of the visual cortex did not find significant HRs in all newborn infants,[4] even though all of them were healthy. In this study, we therefore recorded NIRS and electroencephalography (EEG) simultaneously and over the same cortical location to facilitate the detection of possible reason/s for missing HR.

The aims of this study were (i) to determine the sensitivity and (ii) repeatability of NIRS in response to visual stimulation in healthy newborn infants, (iii) to assess the visual evoked potential (VEP) sensitivity and (iv) repeatability, (v) to screen for optical neuronal signals, and (vi) to identify the possible reason for absent activations in healthy newborn infants.

2 Methods

2.1 Subjects

Demographic data of 14 healthy term newborns are given in Table 1. This study was performed in accordance with the Code of Ethics of the World Medical Association (Declaration of Helsinki) and was approved by the Ethical Committee of the

Address all correspondence to: Martin Biallas, University Hospital Zurich, Frauenklinikstr. 10, 8091 Zurich, Switzerland. Tel.: + 41 44 2555340; Fax: 41 44 2554442; E-mail: martin.biallas@alumni.ethz.ch

Table 1 Demographic information on 14 subjects.

	Mean	SD
At birth		
Gestational age (weeks)	40.4	1.0
Weight (g)	3341	248
Length (cm)	50.0	1.2
Head circumference (cm)	35.0	1.2
Apgar 5′	9	0
Umbilical arterial pH	7.3	0.1
Postnatal		
Age at first measurement (days)	2.1	0.6

Canton of Zurich. Written informed consent was obtained from all parents before inclusion in the study.

2.2 Protocol

Visual flash stimulation was selected because its effectiveness has been shown in the NIRS and the EEG domain.[4,12,13] Subjects underwent visual flash stimulation during sleep held in the arms of a parent. The measurement began shortly after the newborn was fed and lasted 20 min in which rest periods (duration varied randomly between 12 and 32 s) were alternated with stimulation periods of 20 s (Fig. 1). Stimulation consisted of 10-ms-long flashes repeated with 0.5 Hz. The flash device (main wavelength $\lambda = 660$ nm, 600 cd/m^2 at device) was held at a distance of 15 cm in front of the closed eyes of the subject. The EEG electrode O_Z was applied once and was not relocated throughout a measurement. The NIRS sensor, after placement at O_Z, was relocated (10 mm toward C_Z) after 10 min when preliminary data analysis did not indicate a HR, to record a further 10 min. Final NIRS analysis was performed on 20-min recordings, or, when applicable, on the 10-min recording made after sensor relocation. Whether the values of the skin-electrode impedances were in an acceptable range (≤ 40 kΩ) was checked before and after the recording.

2.3 Instrumentation

We used a state-of-the art multichannel photometer developed by our group[14] for optical data recording. This continuous-wave device was configured to switch between four light-source

locations (each able to illuminate tissue at $\lambda = 750$ nm, 800 nm, or 875 nm) and four detectors, arranged as shown in Fig. 2, in order to obtain 11 light paths sampled at 100 Hz.

The EEG was recorded with NicoletOne (VIASYS Healthcare Inc). It utilizes a Tornado V44 amplifier, which records data with 2 kHz sampling frequency. The cutoff frequency of the high-pass filter was 0.01 Hz. Single patient use, Ag/AgCl, solid gel, self-adhesive, foil electrodes were used. The ground electrode was placed at F_Z and the reference electrode at C_Z according to the 10/20-system.[15] Crosstalk and interference were tested for and not found. Light sensor and electrode O_Z were attached as shown in Fig. 2. Electrode O_Z was placed beneath the light sensor. Skin-electrode impedances were kept below 40 kΩ.

2.4 Data Analysis

Evaluation of all acquired data was performed using Matlab. To analyze data for the HR, NIRS raw data was converted into changes of oxyhemoglobin ([O$_2$Hb]) and deoxyhemoglobin ([HHb]) concentration by using the modified Beer-Lambert law.[16] Absorption coefficients were applied as previously described[17] and the differential pathlength factor (DPF) was set to 4.714 at $\lambda = 750$ nm, 4.249 at 800 nm, and 3.5515 at 875 nm.[18] [O$_2$Hb] time intervals were excluded from further analysis when they exceeded 2 μmol/l in a high-pass-filtered (5 pole IIR, $f_c = 0.025$ Hz) copy of the raw trace, because this was considered a movement artifact. After high- and low-pass filtering (high-pass: subtraction of moving average filter, span 40 s; low-pass: least squares smoothing filter, 1 s framesize, first order), the 11 [O$_2$Hb] channels were examined independently with a nonparametric test (Wilcoxon rank sum test) for significant changes ($p < 0.05$) during stimulus onset. For this purpose the data of the time interval from -5 s to stimulus onset (at 0 s) and the interval from 7 to 12 s after the onset were paired for all stimulation periods and used for the statistical test.

EEG raw data was low-pass ($f_c = 100$ Hz, 5 pole Butterworth) and notch filtered at 50 and 100 Hz. Intervals that exceeded 200 μV were excluded from analysis. Based on the preprocessed data, the event-triggered block averages (ETBA) were calculated. ETBAs were determined for stimulation periods and rest periods (sham stimulation) separately. Due to varying latencies of the maximum peak of a VEP, the power of the time interval beginning at 10 ms and ending at 600 ms after stimulation onset during stimulation periods was compared statistically to the same period during sham stimulation. A significant response was defined when power was significantly stronger (Wilcoxon rank sum test, $p < 0.05$) during stimulation than in sham stimulation periods.
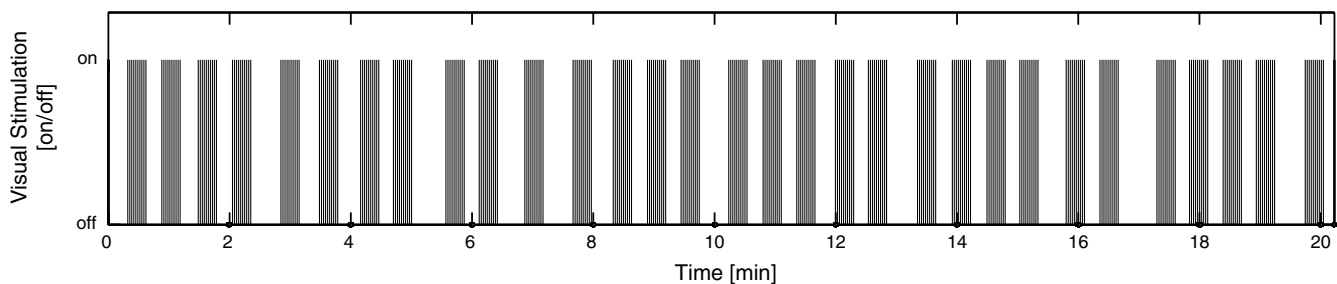

Fig. 1 Stimulation periods over time, with durations of 20 s alternating with rest periods of, in average, also 20 s. Stimulation consisted of 10-ms-long flashes repeated with 0.5 Hz.
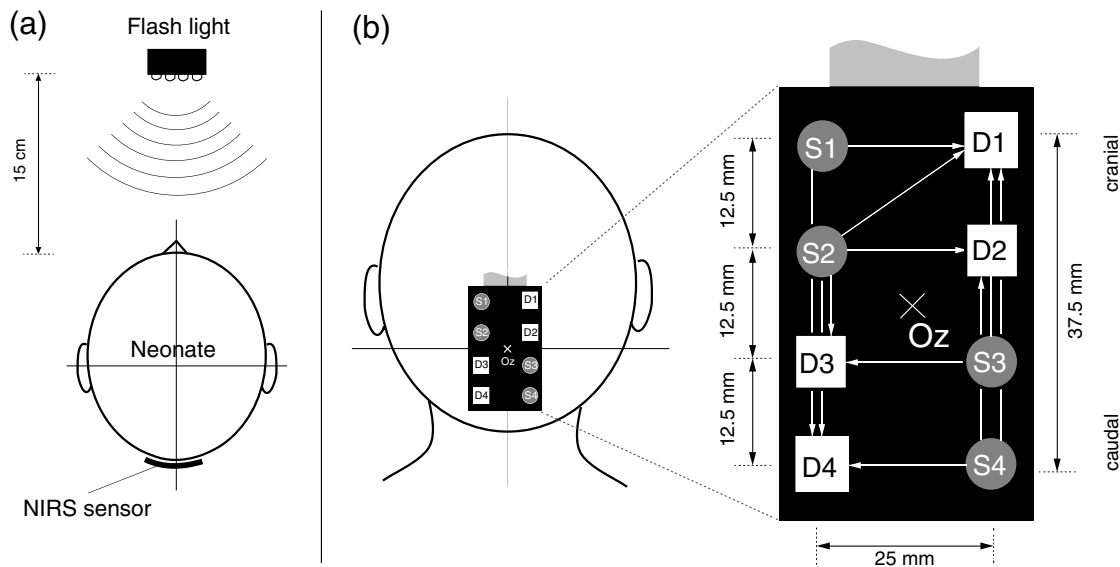
Fig. 2 Attachment and geometry of the light sensor. Light sources/detectors are circles/squares. Each light source can emit light at three different wavelengths. The shortest source-detector distance recorded is 12.5 mm, the longest distance is 37.5 mm. Before the light sensor was attached to the head, a thin foil electrode was placed at position O$_Z$.

Analysis for the optical neuronal signal was performed on logarithmized intensity data normalized by DPF and source-detector distance (in cm) for each channel (i.e. each wavelength of each light path given by a source-detector combination, separately). Since heart beat is known to affect the analysis,[19] a Parameter Estimation of a Model for Almost Periodic Signals (PEMAPS) filter as described in Refs. [20–22] was used to remove heart beat from each channel. One channel per measurement with high signal-to-noise ratio was selected manually as the heart beat reference channel for the PEMAPS filter. To increase the signal-to-noise ratio for the analysis, for each channel and stimulation event the data were segmented from −400 ms before to 1900 ms after an event. Before an ETBA of all stimulation events was calculated, segments exceeding two times the mean variance of all segments were excluded. Afterward the offset of each segment was normalized by subtracting its mean. The same procedure was performed on sham stimulation events. Each sample point given by the ETBAs underwent t-testing ($p < 0.05$) to examine whether its mean value is significantly different from zero. Each significance was transferred into a histogram that showed the number of significant occurrences over time to detect the temporal localization of a potential optical neuronal signal. Assuming that random significances (false positive) appear equally distributed over time, the idea is that stimulation-related significances cluster in a specific time interval after the onset of stimulation. Significant occurrences were collected for stimulation and sham stimulation separately. Furthermore, significances were color coded so that significant negative deviations (black) from zero could be distinguished from positive ones (gray) (see Fig. 3). Such histograms were established for all combinations of available wavelengths and source-detector distances. These combinations were established on the basis of data from a single measurement, a subject, and for the global analysis also over all measurements. An example of histograms over all measurements with a source-detector distance of 12.5 mm and a wavelength of 875 nm is given in Fig. 3. As a control, histograms were plotted for the data before the heart beat was removed by the PEMAPS filter.

The global analysis was based on the normalized noise (standard error of mean [SEM]) distribution of optical density during rest phase after application of PEMAPS. Included were all source-detector distances and wavelengths of all measurements. Occurrences were normalized to the number of light paths used (Fig. 3).

To find out whether a signal qualifies as optical neuronal signal, for the selected source-detector distance of 12.5 mm, it was checked whether four requirements were met: A) Are there more than 60 single events per wavelength? B) Is the temporal evolution of all three wavelengths similar? C) Are three subsets of an ETBA within one wavelength similar? D) Is there a difference in temporal evolution of each wavelength when stimulation periods are compared to rest periods? Criteria B through D are similar to those applied by Franceschini and Boas.[23] All criteria are explained in the following paragraph.

A dataset of segments (containing stimulation events) belonging to a particular channel and wavelength, on which an ETBA was performed, is divided into three subsets. A new ETBA is then calculated on each subset. Criterion C demands that an effect detected by the analysis of an ETBA must also occur in all three subsets. Hence, the result of the ETBA over all segments is considered invalid when the effect does not occur in all of the three subsets. It was defined that a subset has to consist of at least 20 segments to acquire a representative ETBA. This explains why criterion A demands at least 60 stimulation events. Requirements B to D were checked in the time interval from 200 ms to 500 ms after stimulation onset in the selected source-detector distance. To test condition B by linear regression (Pearson), the ETBA of each wavelength was denoised using a moving average filter (window five sample points long); subsequently, the filtered ETBA segments underwent regression. When all squared correlation coefficients (r^2) of the regression's matrix (dimension 3×3, one wavelength for each row and column) were greater or equal to 0.5, B was fulfilled. To examine condition C, the equality of subsets, differences between all combinations of the three subsets were calculated leading to a new 3×3 matrix consisting of p values from t-testing ($p < 0.05$) distributions of differences of each
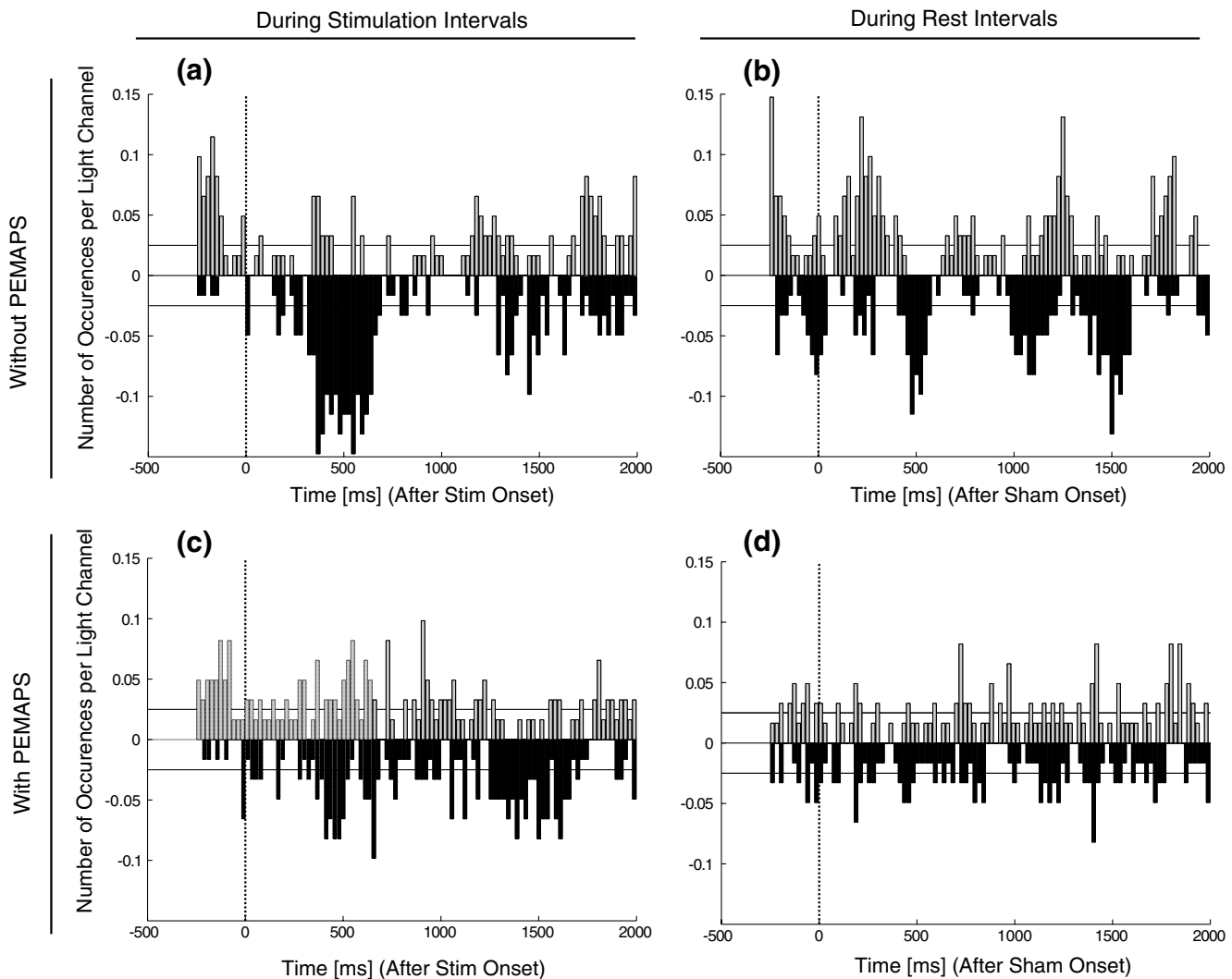
Fig. 3 Histograms of significant changes in intensity compared to baseline. The y-axis indicates the number of significant changes detected divided by the total number of measurements at this specific period of time (x-axis). For a significance level of $p = 0.05$ it is expected that every 20th measurement is significant just due to chance (i.e., at a probability of 0.05). Since we have separated positive and negative changes in intensity, the probability of a significance occurring just by chance is 0.05/2. This level of false positive significance has been indicated by horizontal lines in the histogram. For better visualization number of occurrences of significant negative deviations is depicted as negative values. These histograms show the light path defined by 875 nm and 12.5 mm source-detector distance of all measurements, without heart beat filtering (PEMAPS) (a,b) and after application of PEMAPS (c, d). Left: Accumulation of significances at 400 to 500 ms and around 1500 ms after stimulation onset at 0 ms. Right: Accumulation is less pronounced during rest intervals (sham stimulation).

subset combination against 0. C was met when no t-test of unequal subsets showed a significant difference to 0. Finally, condition D, the difference between stimulation and rest phases, was tested by subtracting stimulation and sham stimulation ETBAs per wavelength. If the t-test ($p < 0.05$) of a difference was significantly different from 0 for all wavelengths, then constraint D was regarded fulfilled. The findings for the criteria A to D per measurement are given in Table 2.

3 Results

Under the assumption that visual stimulation was only successful when there was a detectable VEP response, (i) a HR was detected in 61.5% of all measurements (16 significant responses in 26 measurements), and (ii) 11 HRs were associated with an increase in $[O_2Hb]$, while five cases showed the contrary effect. In 41.7% a HR could be detected in both measurements within a

subject (5 of 12 subjects). An event-triggered median trace of a successful HR is presented in Fig. 4.

EEG analysis resulted in (iii) a sensitivity of 96.3% (26 VEPs in 27 measurements) when assuming successful stimulation in all measurements. The 28th measurement could not be analyzed for technical reasons and was excluded. A measurement with a negative power difference of its VEP in comparison to rest periods was considered unsuccessful. (iv) In 12 of 13 subjects a significant VEP could be found in both sessions (92.3%). The VEP of a successful stimulation is shown in Fig. 5.

Regarding the optical neuronal signal, a global analysis over all measurements was performed. It was found that (v) the global noise level (SEM) over all measurements was $P_{20} = 9.6 \times 10^{-5}\%$ in changes of optical density.

Global analysis further revealed a decrease in optical density before 500 ms after stimulation onset, in all three wavelengths. This was most pronounced in source-detector distances of

Table 2 Overview of subjects and result of analysis.

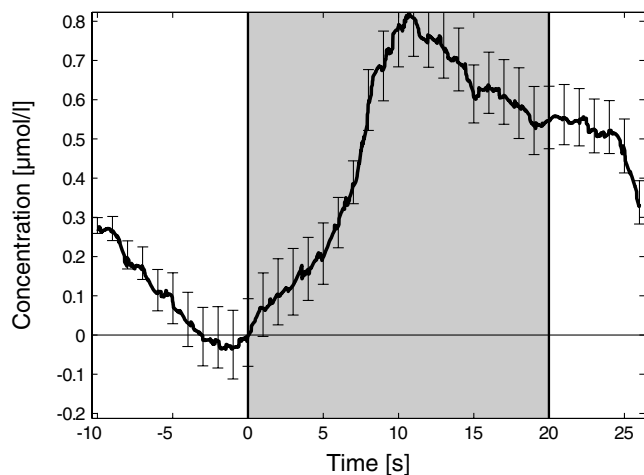| Subject index	Gender	Gestational age [weeks+days]	Recording index	Postnatal age [days]	Duration of recording [min]	P value HR	HR Δ mean [mol/l]	VEP Δ mean [nW]	A) Number of segments ≥60	B) Similar temporal evolution of all 3 wavelenghts	C) Subsets within one wavelength equal	D) Difference between stimulation and rest
1	F	40 + 3	A	2	20	0.0045	1.22 ± 0.47	15.6 ± 0.02	Y	N (Y)	N (Y)	N (Y)
			B	3	20	0.0469	−0.56 ± 0.19	1.8 ± 0.01	na	na (na)	na (na)	na (na)
2	M	40 + 2	A	1	20	0.0438	0.35 ± 0.15	23.1 ± 0.02	Y	N (N)	N (N)	N (N)
			B	4	10	0.0353	0.37 ± 0.17	8.0 ± 0.01	Y	N (N)	N (N)	N (N)
3	M	40 + 1	A	4	20	—	—	−0.6 ± 0.01	Y	N (N)	N (N)	N (N)
			B	5	10	—	—	0.5 ± 0.01	N	N (N)	N (N)	N (N)
4	F	41 + 2	A	2	20	—	—	10.2 ± 0.02	Y	Y (Y)	N (N)	N (Y)
			B	3	20	—	—	8.1 ± 0.01	Y	N (Y)	N (N)	N (N)
5	F	41 + 4	A	2	10	0.0400	0.76 ± 0.31	4.7 ± 0.01	Y	Y (Y)	Y (Y)	Y (Y)
			B	3	20	—	—	13.5 ± 0.02	N	Y (Y)	N (N)	N (N)
6	M	38 + 5	A	2	10	0.0005	2.99 ± 0.68	13.6 ± 0.02	Y	Y (Y)	N (N)	Y (Y)
			B	3	10	0.0479	0.71 ± 0.32	—	Y	Y (Y)	Y (Y)	Y (Y)
7	M	41 + 2	A	2	20	<0.0001	2.46 ± 0.42	8.5 ± 0.01	Y	Y (Y)	N (N)	Y (Y)
			B	3	20	0.0230	−0.75 ± 0.33	1.4 ± 0.01	Y	N (N)	N (N)	N (N)
8	M	40 + 0	A	2	10	—	—	24.1 ± 0.03	Y	Y (Y)	N (N)	Y (Y)
			B	3	10	0.0256	0.25 ± 0.10	2.3 ± 0.01	Y	N (N)	Y (Y)	Y (Y)
9	F	41 + 2	A	2	10	—	—	2.1 ± 0.01	N	Y (Y)	Y (Y)	N (N)
			B	3	20	—	—	15.7 ± 0.02	Y	N (Y)	N (N)	Y (Y)
10	M	40 + 1	A	2	20	0.0449	−0.84 ± 0.40	2.7 ± 0.01	Y	Y (Y)	N (N)	N (N)
			B	4	20	—	—	2.4 ± 0.01	N	N (N)	N (N)	Y (Y)
11	M	41 + 3	A	2	10	0.0065	1.07 ± 0.29	3.8 ± 0.01	Y	Y (Y)	N (N)	N (Y)
			B	3	20	0.0322	1.01 ± 0.41	18.1 ± 0.01	Y	Y (Y)	N (N)	Y (Y)
12	M	41 + 4	A	2	20	0.0177	−0.22 ± 0.08	5.4 ± 0.01	Y	Y (Y)	Y (Y)	N (N)
			B	3	20	0.0093	−0.69 ± 0.27	3.5 ± 0.01	Y	Y (Y)	Y (Y)	N (N)
13	F	38 + 3	A	2	10	—	—	82.6 ± 0.12	Y	N (N)	N (N)	Y (Y)
			B	3	20	0.0065	1.35 ± 0.46	56.3 ± 0.07	Y	N (N)	N (N)	N (N)
14	M	39 + 1	A	2	20	0.0270	0.25 ± 0.14	3.1 ± 0.01	Y	Y (Y)	N (N)	Y (Y)
			B	3	20	—	—	10.5 ± 0.02	Y	N (N)	N (N)	Y (Y)

Fig. 4 Grand average of all significant $[O_2Hb]$ hemodynamic responses. Stimulation begins at 0 s and ends at 20 s. An increase of $[O_2Hb]$ can be seen after stimulation onset. The standard error of mean is depicted by error bars.

12.5 mm [compare Fig. 3(c) and 3(d)], smaller with 25 mm, and not detectable with 35 mm. Table 2 provides the information about which measurements met requirements to qualify the signal as an optical neuronal signal. One measurement could not be analyzed due to low signal-to-noise ratio in heart beat reference channel, which led to fragmented filtered data. In summary, 23 out of 27 measurements ($\hat{=}85.2\%$) provided a sufficient number of stimulation events to continue the analysis. Of these, two measurements fulfilled the requirements for an optical neuronal signal. There two occurred in different subjects and were not reproducible. (vi) Insufficient stimulation was ruled out as reason for absent HRs as VEPs were present.

4 Discussion

4.1 Hemodynamic Response

The sensitivity of NIRS in this study is 61.5%. Although NIRS is a potentially powerful method for studying brain activity in newborns, so far, its sensitivity is not high enough for clinical applications. This result is in accordance with the review by Wolf and Greisen,[4] who concluded that effects are often only
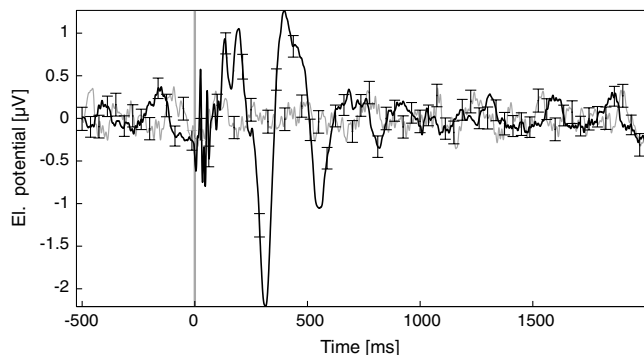

Fig. 5 Grand average of all triggered block averages (ETBA) of visual evoked potentials. Stimulation event is at 0 ms. The trace depicting the ETBA during rest is related to sham stimulation events at 0 ms. While the trace belonging to the stimulation events shows clear deviations from zero, the rest trace is steady. The standard error of mean is depicted by error bars.

seen in group averages. Several possibilities can contribute to the absence of HRs: for example, (i) an insufficient stimulation unable to activate the brain, (ii) an immature brain unable to respond to the stimulus, (iii) a NIRS measurement not localized at the relevant cortical position of brain activity, and (iv) an insufficient change in HR despite an activation. In the present study, by verifying the cerebral response with EEG, (i) and (ii) were excluded noticing that indeed, using lower luminance for stimulation lead to less VEPs in the data.[24] For three subjects (see Table 2) in whom HRs were absent while EEG showed significant responses, reasons (iii) and (iv) could be claimed. Nevertheless, there were five subjects in whom a HR was detected only once, for whom (iii) and (iv) cannot be applied. Further differentiation for the remaining reasons (iii) and (iv) is not possible based on the data acquired here.

The value found for NIRS sensitivity here is slightly higher compared to the study presented by Karen et al.[11] where 50% sensitivity was achieved for $[O_2Hb]$. Reasons for the improvement may lie in the relaxed demand on the p value ($p < 0.05$ in contrast to $p < 0.01$), and in utilizing a more intense light for visual stimulation (600 cd/m^2). In 10 of 28 (35.7%) measurements the NIRS sensor was moved toward C_Z after 10 min, leading in six measurements to a significant HR. Although EEG electrodes were never relocated, the sensitivity for the VEP was high (see Visual Evoked Potential below).

Determining the relative $[O_2Hb]$ concentration by the DPF method (or, in other words, the modified Beer-Lambert) requires the following assumptions: a specific value of the DPF and that a change in the concentration is homogeneous across the illuminated volume of tissue. Concerning the first assumption, the values for a different DPF can be easily calculated by multiplying our numbers by the DPF applied by us and then dividing them by a different DPF. The second assumption is not fulfilled in our case, because functional changes in $[O_2Hb]$ concentration occur locally. This leads to an underestimation of the amplitudes of the local changes in perfusion. This effect has previously been described in detail.[25,26] Since in neonates the thickness of skin and skull is much smaller compared to that in adults, this error is smaller.

Future measurements should consider covering a larger area with the NIRS sensor, to avoid relocating.

4.2 Visual Evoked Potential

Due to the biphasic nature and varying latencies of the response in the EEG, it was tested whether the power during stimulation was significantly greater than during rest period (sham stimulation). In 96.3% a VEP was detected. In the literature, sensitivity of 100% can be found.[13] Although our data analysis underwent a more stringent approach, by comparing stimulation and rest periods, than the one by Benavente et al.,[13] the results are similar. Of the two measurements that did not lead to a significant response, one could not be analyzed for technical reasons. The other one was excluded as successful response, as the power during stimulation periods was smaller than the power during rest periods.

4.3 Optical Neuronal Signal

To detect the temporal localization of a potential optical neuronal signal, histograms showing the occurrences of significant deviations from 0 were employed. Histograms included all measurements and combinations of different source-detector
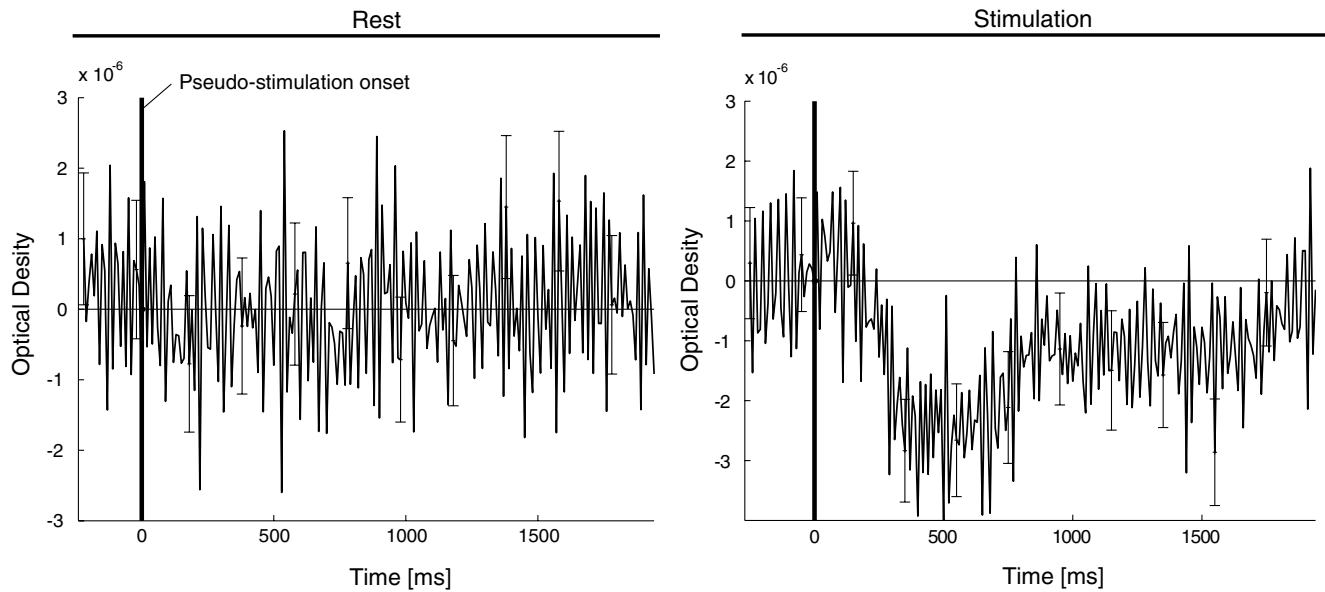
Fig. 6 Event-triggered block average (ETBA) of optical density for one measurement and one light path thereof: 750 nm, 12.5 mm source-detector distance, after application of heart beat filter (PEMAPS). Left: ETBA during rest interval (sham stimulation). Right: ETBA during stimulation. (Sham-) stimulation event is at 0 ms. During stimulation a significant decrease in intensity is visible at approximately 500 ms, which is likely to constitute an optical neuronal signal. The SEM is depicted by error bars.

distances and wavelengths. The first set of histograms showed an accumulation of significances in the time interval of approximately 400 to 500 ms after stimulation onset, most pronounced for the source-detector distance of 12.5 mm (see Fig. 3) and less clear for 25 mm and 37.5 mm, in all wavelengths. With this information the next step in the analysis was to test whether data with 12.5-mm source-detector distance of each single measurement met criteria to qualify as an optical neuronal signal. The three main criteria were, (B) equal temporal evolution in all wavelengths, (C) equal subsets in ETBA, and (D) difference between stimulation and rest (sham stimulation). Criterion (B) implies that there is no characteristic spectrum of a potential optical neuronal signal in the spectrum employed here. This assumption holds true when changes in scattering are the source of intensity changes, as suggested in previous studies.[23,27–29]

Table 2 lists the results for each criterion and measurement. Two measurements met all criteria after application of PEMAPS (three without). A single ETBA, characteristic for all three wavelengths and the two significant measurements, is shown in Fig. 6. These two measurements show signal changes of optical density in the order of $<10^{-3}\%$. Literature on the magnitude of changes in optical density of an optical neuronal signal is not available for newborns. On the other hand, in adults values for changes in light intensity range from 0.01% to 0.00001%.[29] The effect found here is about 63 times larger than the lower boundary of this given range for adults (assumption is DPF = 4.714 and distance 1.25 cm). The increased effectiveness of NIRS in newborns is also shown in simulations.[30] The P_{20} noise level achieved over all measurements is $9.6 \times 10^{-5}\%$ in units of changes in optical density. The complete noise distribution is depicted in Fig. 7.

Accumulation of significances are present in histograms that have the heart beat not removed [Fig. 3(a)]. Interestingly, after filtering the data with PEMAPS, the effect remains visible in the histogram representing stimulation periods, whereas during rest there is no clear effect. However, various reasons for this phenomenon can be excluded. Direct coupling of the light for

stimulation into the light sensors' detector would appear in the range of 0 ms to 10 ms in histograms. Heart beat artifacts can be excluded because with heart beat rates in newborns of above 100 bpm, they would appear several times within the 2 s interval between two stimulation events. Movement artifacts are also unlikely since they would have an impact on all other lightpaths.

When the two significant measurements are removed from the histograms, there is no more clear clustering of significances. One possible reason for detecting the optical neuronal signal only twice is insufficient signal-to-noise ratio. The small margin of the optical neuronal signal in comparison to noise
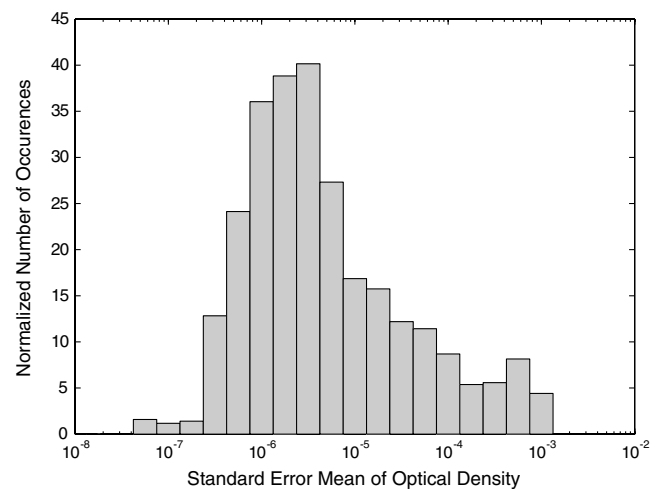

Fig. 7 Histogram of normalized noise (SEM) distribution of optical density during rest phase after application of PEMAPS. Included are all source-detector distances and wavelengths of all measurements. Occurrences were normalized to the number of light paths used. Notice: SEM of optical density is not given in %. This histogram shows that many measurements achieve extremely low noise.

leads to an increase of susceptibility to parameters like the thickness of skin and skull and their optical density. A further impact on the signal-to-noise level has the course of a measurement. When the sleep of a newborn is fitful, the number of artifacts increases, and by subsequent exclusion in data processing the signal-to-noise ratio decreases.

To the knowledge of the authors, this is the first study assessing reproducibility of NIRS to photic stimulation in newborns, and that screens the data for potential optical neuronal signals.

5 Conclusion

The sensitivity of NIRS to detect the hemodynamic response is 61.5%, which is comparable to previous findings. Aside from sensitivity, it was shown that the hemodynamic activation can be reproduced in 41.7% of all subjects.

Sensitivity of the EEG is 96.3% and can be reproduced in 92.3% of all subjects. Thus, in this study we can exclude that HR was absent due to insufficient activation.

Two measurements met all criteria for the identification of an optical neuronal signal, which could however not be reproduced, despite the noise achieved ($P_{20} = 9.6 - 10^{-5}\%$ in change of optical density). In summary, this study shows the importance of using control data from sham stimulation intervals and from non–heart beat-filtered data to avoid false positive identification of optical neuronal signals. Although NIRS is a promising research method to examine brain function noninvasively, the low sensitivity and reproducibility regarding detection of HRs and of responses of potential optical neuronal signals render its introduction in clinical procedures difficult. This study demonstrates that NIRS and EEG can be measured in parallel in newborn infants.

References

1. M. O'Reilly et al., "Ophthalmological, cognitive, electrophysiological and MRI assessment of visual processing in preterm children without major neuromotor impairment," *Dev. Sci.* **13**(5), 692–705 (2010).
2. B. Hout et al., "Relation between visual perceptual impairment and neonatal ultrasound diagnosis of haemorrhagic-ischaemic brain lesions in 5-year-old children," *Dev. Med. Child Neurol.* **42**(6), 376–386 (2000).
3. M. G. Torrioli et al., "Perceptual-motor, visual and cognitive ability in very low birthweight preschool children without neonatal ultrasound abnormalities," *Brain Develop.* **22**(3), 163–168 (2000).
4. M. Wolf and G. Greisen, "Advances in near-infrared spectroscopy to study the brain of the preterm and term neonate," *Clin. Perinatol.* **36**(4), 807–834 (2009).
5. T. Kono et al., "Multiple-time replicability of near-infrared spectroscopy recording during prefrontal activation task in healthy men," *Neurosci. Res.* **57**(4), 504–512 (2007).
6. M. Plichta et al., "Event-related functional near-infrared spectroscopy (fNIRS): are the measurements reliable?," *NeuroImage* **31**(1), 116–124 (2006).
7. Y. Hoshi et al., "Hemodynamic responses to photic stimulation in neonates," *Pediatr. Neurol.* **23**(4), 323–327 (2000).
8. T. Kono et al., "Multiple-time replicability of near-infrared spectroscopy recording during prefrontal activation task in healthy men," *Neurosci. Res.* **57**(4), 504–512 (2007).
9. J. Meek et al., "Regional hemodynamic responses to visual stimulation in awake infants," *Pediatr. Res.* **43**(6), 840–843 (1998).
10. G. Taga et al., "Hemodynamic responses to visual stimulation in occipital and frontal cortex of newborn infants: a near-infrared optical topography study," *Pathophysiology* **10**(3–4), 277–281 (2004).
11. T. Karen et al., "Hemodynamic response to visual stimulation in newborn infants using functional near-infrared spectroscopy," *Hum. Brain Mapp.* **29**(4), 453–460 (2008).
12. J. Mushin et al., "The visual evoked potential in neonates with occipital lesions and holoprosencephaly," *Behav. Brain Res.* **21**(2), 79–83 (1986).
13. I. Benavente et al., "Flash visually evoked potentials in the newborn and their maturation during the first six months of life," *Doc. Ophthalmol.* **110**(2), 255–263 (2005).
14. D. Haensse et al., "A new multichannel near infrared spectrophotometry system for functional studies of the brain in adults and neonates," *Opt. Express* **13**(12), 4525–4538 (2005).
15. H. H. Jaspers, "Report of the committee on methods of clinical examination in electroencephalography: 1957," *Electroen. Clin. Neuro.* **10**(2), 370–375 (1958).
16. L. Kocsis, P. Herman, and A. Eke, "The modified Beer–Lambert law revisited," *Phys. Med. Biol.* **51**(5), N91–N98 (2006).
17. S. Wray et al., "Characterization of the near infrared absorption spectra of cytochrome aa3 and haemoglobin for the non-invasive monitoring of cerebral oxygenation," *Biochim. Biophys. Acta (BBA)—Bioenergetics* **933**(1), 184–192 (1988).
18. C. E. Cooper et al., "The noninvasive measurement of absolute cerebral deoxyhemoglobin concentration and mean optical path length in the neonatal brain by second derivative near infrared spectroscopy," *Pediatr. Res.* **39**(1), 32–38 (1996).
19. G. Gratton and P. Corballis, "Removing the heart from the brain: compensation for the pulse artifact in the photon migration signal," *Psychophysiology* **32**(3), 292–299 (1995).
20. I. Trajkovic et al., "Modelling and filtering almost periodic signals by time-varying fourier series with application to near-infrared spectroscopy," in *Proc. 17th European Signal Proc. Conf. (EUSIPCO)*, Glasgow, pp. 632–636 (2009).
21. I. Trajkovic, C. Reller, and M. Wolf, "Modelling and filtering of physiological oscillations in near-infrared spectroscopy by time-varying Fourier series," in *Proc. International Society on O2 Transport to Tissue (ISOTT)*, pp. 307–313Springer, New York (2012).
22. I. Trajkovic, "Modelling and filtering almost periodic signals by time-varying Fourier series with application to near-infrared spectroscopy," Ph.D. Thesis, Diss ETH No 19420 ETH Zurich (2010).
23. M. Franceschini and D. Boas, "Noninvasive measurement of neuronal activity with near-infrared optical imaging," *NeuroImage* **21**(1), 372–386 (2004).
24. M. Biallas et al., "How to conduct studies with neonates combining near-infrared imaging and electroencephalography," *Oxygen Transport to Tissue XXXIII*, pp. 111–117, Springer, New York (2012).
25. E. Okada et al., "Theoretical and experimental investigation of near-infrared light propagation in a model of the adult head," *Appl. Opt.* **36**(1), 21–31 (1997).
26. D. Boas et al., "The accuracy of near infrared spectroscopy and imaging during focal changes in cerebral hemodynamics," *NeuroImage* **13**(1), 76–90 (2001).
27. M. Kubota et al., "Fast (100-175 ms) components elicited bilaterally by language production as measured by three-wavelength optical imaging," *Brain Res.* **1226**, 124–133 (2008).
28. A. Villringer and B. Chance, "Non-invasive optical spectroscopy and imaging of human brain function," *Trends Neurosci.* **20**(10), 435–442 (1997).
29. M. Wolf et al., "Near infrared spectroscopy to study the brain: an overview," *Opto-Electron. Rev.* **16**(4), 413–419 (2008).
30. Y. Fukui, Y. Ajichi, and E. Okada, "Monte Carlo prediction of near-infrared light propagation in realistic adult and neonatal head models," *Appl. Opt.* **42**(16), 2881–2887 (2003).